Stable microfluidic flow focusing using hydrostatics[a]

Vaskar Gnyawali,[1, 2, 3] Mohammadali Saremi,[1, 2, 3] Michael C. Kolios,[2, 3, 4] and Scott S. H. Tsai[1, 2, 3, b]

[1] *Department of Mechanical and Industrial Engineering, Ryerson University, Toronto, Canada*

[2] *Institute for Biomedical Engineering, Science and Technology (iBEST), Toronto, Canada*

[3] *Keenan Research Centre, St. Michaels Hospital, Toronto, Canada*

[4] *Department of Physics, Ryerson University, Toronto, Canada*

(Dated: 25 April 2017)

We present a simple technique to generate stable hydrodynamically focused flows by driving the flow with hydrostatic pressure from liquid columns connected to the inlets of a microfluidic device. Importantly, we compare the focused flows generated by hydrostatic pressure and classical syringe pump driven flows, and find that the stability of the hydrostatic pressure driven technique is significantly better than the stability achieved via syringe pumps, providing fluctuation-free focused flows that are suitable for sensitive microfluidic flow cytometry applications. We show that the degree of flow focusing with the hydrostatic method can be accurately controlled by the simple tuning of the liquid column heights. We anticipate that this approach to stable flow focusing will find many applications in microfluidic cytometry technologies.

---

[a] Footnote to title of article.

[b] Electronic mail: scott.tsai@ryerson.ca

I. INTRODUCTION

The development of microfluidic techniques in recent years is leading to an emergence of enhanced lab-on-a-chip (LOC) devices.[1,2] Such LOC devices demonstrate the potential of replacing existing larger scale technologies in bio-chemical, bio-physical, and bio-medical processes.[3–5] A major advantage of LOC devices is the ability to provide a quasi-natural environment to cells that are under observation by controlling flow properties such as laminarity,[6,7] physical parameters such as flowrate,[7,8] and the size of the microchannels.[7] The application of hydrodynamic focusing in these microfluidic flows provides an additional advantage by narrowing the flows toward the size of a single cell.[9] For example, in a flow cytometer,[10] single cells are hydrodynamically flow focused to a narrow stream that passes through an interrogating zone where the individual cells are interrogated by optical[11] or electrical systems[12,13] for diagnostics and sorting applications. In addition to flow cytometry, focused flows are also useful in applications such as drug discovery,[14,15] drug delivery and release,[14] deoxyribonucleic acid (DNA)-stretching,[16] and reagent mixing in microfluidics.[17]

Typical microfluidics experiments use constant flow-rate syringe pumps to drive the fluid flow.[5] The flows generated by syringe pumps visually appear to be precise,[18] but measurements show that the diameter of focused flows from syringe pumps can fluctuate significantly: one recent publication shows radial variation of 13 μm when the average diameter is 217 μm.[19] The authors detect the fluctuations of syringe pumps by tracking the interface of ultralow interfacial tension aqueous two phase systems (ATPS) and demonstrate that the fluctuations are directly related to the steps of the stepper motor in the pumps. In a similar approach, another publication shows that the flow fluctuations are related to the pressure fluctuations in the syringe pumps.[20] These syringe pumps also produce periodic oscillations in the flows due to the frictional forces between the syringe piston and the syringe wall.[21]

These flow instabilities caused by syringe pumps may have a detrimental effect on the effectiveness of new and highly sensitive microfluidic flow cytometry methods.[22] Indeed, the requirements for narrow and consistent flow focusing in these newly developed microfluidic flow cytometry techniques are highlighted in a recent publication by Strohm *et al.*,[23] where the researchers are attempting to characterize cells and particles using acoustics in microfluidics.

In this paper, we demonstrate the application of hydrostatic pressure-driven flow to

achieve precise and stable flow focusing. We compare experimental results from hydro-statics and syringe pump-driven flow focusing and find that hydrostatics achieves superior flow focusing stability in a range of focused widths. Finally, we show that our hydrostatics-based flow focusing technique is easily tunable to control the width of the focused flow. We anticipate that this stable and easily tunable hydrostatics-based flow focusing method will find utility in many sensitive microfluidic flow cytometry applications that require highly stable focused flows.

II.   EXPERIMENTAL METHODS

A.   Device fabrication

The microfluidic devices in our experiments are fabricated using the classical soft lithog-raphy technique.[24] A photomask is designed using computer-aided design (CAD) software (AutoCAD 2010, Autodesk, Inc., Dan Rafael, CA, USA), printed on a transparency sheet (25,400 dpi, CAD/ART Services Inc., Bandon, OR, USA), and patterned on a silicon wafer in a single SU-8 layer using photolithography. The pattern is transferred to a polydimethyl-siloxane (PDMS, Sylgard 184 silicone elastomer kit, Dow Corning, Midland, MI, USA) sheet. Inlet and outlet holes on the PDMS base are opened using a 1 mm diameter biopsy punch (Integra Miltex, Inc., Rietheim-Weilheim, Germany). The PDMS sheet is then bonded to a glass microscope slide by oxygen plasma treatment (Harrick Plasma, Ithaca, NY, USA).

Upstream of the flow focusing cross-junction, the sheath flow channels and the sample channel are 100 and 200 μm wide, respectively (Fig. 1a). The channel downstream of the cross-junction is $w = 300$ μm wide (Fig. 1a). The height of all channels is $h = 300$ μm. To obtain flow focusing, a nano-needle (ID = 100 μm, OD = 200 μm; Japan Bio Products, Tokyo, Japan) is manually guided through the sample inlet channel up to the cross junction (Fig. 1b). After inserting the needle, we align the needle in the lateral direction under a stereo microscope (E-Zoom 6V, Edmund Optics Inc., Barrington, NJ, USA). For vertical positioning, we place two layers of a thin transparent tape (3M, St. Paul, MN, USA) underneath the needle to achieve a 40 μm gap between the needle and the bottom of the channel, resulting in a 60 μm gap above the needle. The sheath flows, above and below the sample flow, cause an axis-symmetric effect on the focused flow in both lateral (x-y)

and vertical (x-z) axes (see the supplementary video). Finally, the needle is bonded to the glass substrate and the guiding channel is sealed using two-component epoxy glue (Henkel Canada Corporation, Mississauga, ON, Canada). To connect the needle inlet to the liquid columns, we bind the outer end of the needle to Tygon tubing using the two-component epoxy glue.

B.   Experimental setup

To drive the flow inside the microchannels, we introduce liquid columns containing the sample and sheath fluids. The hydrostatic pressure due to the liquid columns drives the sample and sheath flows. Measuring pipettes (Corning Inc., Corning, NY, USA) with internal diameters 3 mm and 8 mm are used as sample and sheath liquid columns, respectively. The tapered end of the measuring pipettes are inserted into pre-fabricated PDMS cubes, and Tygon tubing is used to connect the cubes to the inlets of the microfluidic devices (Fig. 1a). The sample and sheath flow liquid columns have heights H_1 and H_2, respectively. To compare the results from hydrostatics-based flow focusing with classical syringe pump based flow focusing, we also perform experiments using the same microfluidic geometries with Pump 11 Elite syringe pumps (Harvard Apparatus, Holliston, MA, USA).

We use permanent black ink (Higgins, Chartpak Inc., Leeds, MA, USA) as sample fluid and deionized (DI) water as sheath fluid for all of our experiments. The ink is filtered through a syringe filter (Corning Inc., Corning, NY, USA), with 0.45 μm diameter pores. The color contrast between the ink and the DI water provides clear visualization of the focused sample flow. Fig. 1d is a representative experimental image of the flow focusing of a narrow sample fluid in our microfluidic system. Here, we include 3 μm diameter polystyrene particles in the sample fluid to further enhance the imaging contrast.

The focused flow is imaged using a high-speed camera (Phantom M110, Vision Research, Wayne, NJ, USA) attached to an inverted microscope (Olympus Corporation, Tokyo, Japan). For all of the experiments, the objective is focused at a region approximately 15 mm downstream of the cross-junction. We measure the focused flow diameter, d_s, at the same location in the microchannel for all of our experiments. We use an in-house Matlab program to extract individual frames from the videos and analyze the intensity of each pixel in each frame. The program uses the intensity values to measure the focused flow diameter,
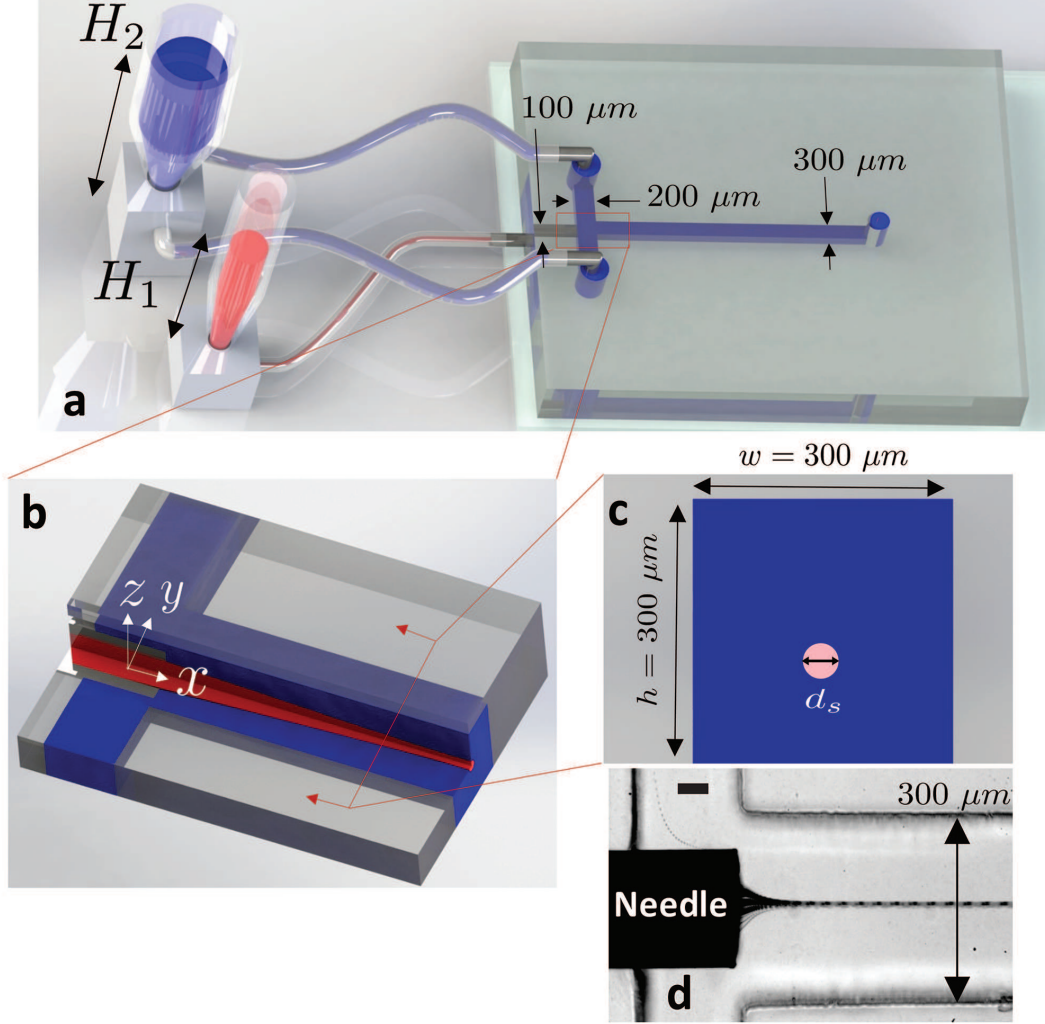
4

FIG. 1. The hydrostatics-based microfluidic device. Schematic illustrations show that (a) fluid flow is driven by hydrostatic pressure that is controlled by the liquid column heights H_1 and H_2 of the sample (red) and sheath (blue) liquids, respectively. The sample flow is supplied to the microchannel via a needle that is inserted to the side of the PDMS slab and the sheath flow enters the microchannel via tubing connected from the top of the device. (b) Extended isometric section view of the flow focusing cross-junction shows that the sheath flow surrounds and flow focuses the sample flow. Sample and sheath fluids both flow in the direction indicated by the x-axis. (c) Cross section view of the microchannel downstream of the cross-junction shows the diameter, d_s, of the flow of the sample fluid. Experimental image showing (d) the flow focusing of the sample fluid near the cross junction. Scale bar represents 50 μm.

d_s, for on each individual frame and calculate the average focused flow diameter. We use the Otsu greyscale thresholding algorithm for intensity thresholding in the frames.[25]

III.   RESULT AND DISCUSSION

A.   The stability of hydrostatics and syringe pump based flow focusing

In our comparison of hydrostatics and syringe pump based microfluidic flow focusing, we use a baseline sample flow diameter, $d_s = 59$ μm, to compare the stability of both systems under equally narrow flow focusing requirements. To attain the focused flow diameter, $d_s = 59$ μm, we apply sample and sheath liquid column heights, $H_1 = 149$ mm and $H_2 = 48$ mm, respectively, in the hydrostatics experiment, and sample and sheath flow rates, $Q_1 = 1.5$ μL/min and $Q_2 = 30$ μL/min, respectively, in the syringe pump experiment.

Fig. 2 shows representative sequential images from the same section of the focused sample flow taken from experimental videos. These sequential images are extracted at an interval of 50 ms apart. The dark sections indicate the sample flow, and the bright sections represent the sheath fluid. Figs. 2a and 2b are bright field images and Figs. 2c and 2d are the binary version of the same images after the Otsu thresholding.

The experimental thresholded images from hydrostatics based focusing (Fig. 2c) shows a consistent focused diameter d_s, both spatially and temporally, in comparison with the thresholded images from syringe pump experiments (Fig. 2d). Additionally, the syringe pump based focused flow exhibits more erratic behavior. For example, the frame taken at 100 ms shows the focused flow tilting on an angle relative to the longitudinal axis of the flow. As hypothesized in previous reports on microfluidic flows with syringe pumps, the variation of the focused width in the syringe pump experiments may arise from the pulsation of the stepping mechanism in the pumps,[19,20] and the tilted focused flow may be due to stiction between the syringe piston and the syringe walls.[21]

For a quantitative comparison of the stability of the focused flows from the two experimental setups, we plot the focused sample flow diameter, d_s, versus time, t (Fig. 3). Here, the average focused flow diameter $d_s = 59$ μm. Blue triangles show experimental data from hydrostatics experiments, and red diamonds show data from syringe pump based experiments. Fig. 3 demonstrates that hydrostatics based flow focusing results in consistently
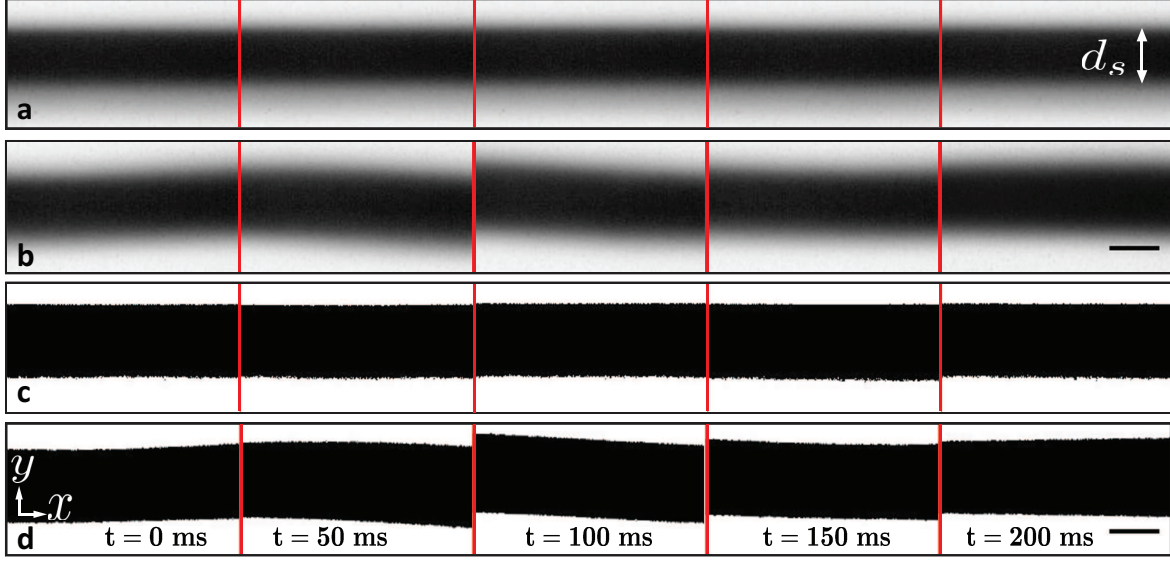
FIG. 2. Experimental images of the sample fluid (black) focused inside a microchannel downstream of the focusing junction. These images are taken from video frames of the experiments whose focused flow average diameter, $d_s = 59$ μm, and the frames are selected at an interval of 50 ms. Brightfield images of the focused flows controlled by (a) hydrostatic pressure and (b) constant flow-rate syringe pumps. Thresholded images of the same focused flows produced with (c) hydrostatic pressure and (d) constant flow-rate syringe pumps. The image sequences show qualitatively that the hydrostatics-controlled focused flow has a more consistent diameter, d_s, than syringe pump driven flow. Syringe-pump driven focused flows also exhibit more erratic flow behavior. Flow is in the direction indicated by the x-axis. Scale bars represent 50 μm.

lower variation of the focused flow diameter, d_s, when compared to syringe pump based experiments. The standard deviation of the focused flow diameter, d_s, is 0.685 μm for hydrostatics, versus 1.589 μm for the syringe pump experiment.

Fig. 4 shows a plot of the cumulative distribution function of the dimensionless focused flow diameter, d_s/w, for cases where $d_s/w = 0.075$, 0.100, 0.140 and 0.197. Here, blue dashed lines show data from hydrostatics experiments and red solid lines show data from syringe pump experiments. Black solid vertical lines indicate the mean values of d_s/w. The distribution of the focused flow diameter is measured from individual diameters of the focused flow in each frame of the videos taken from the experiments. For hydrostatics
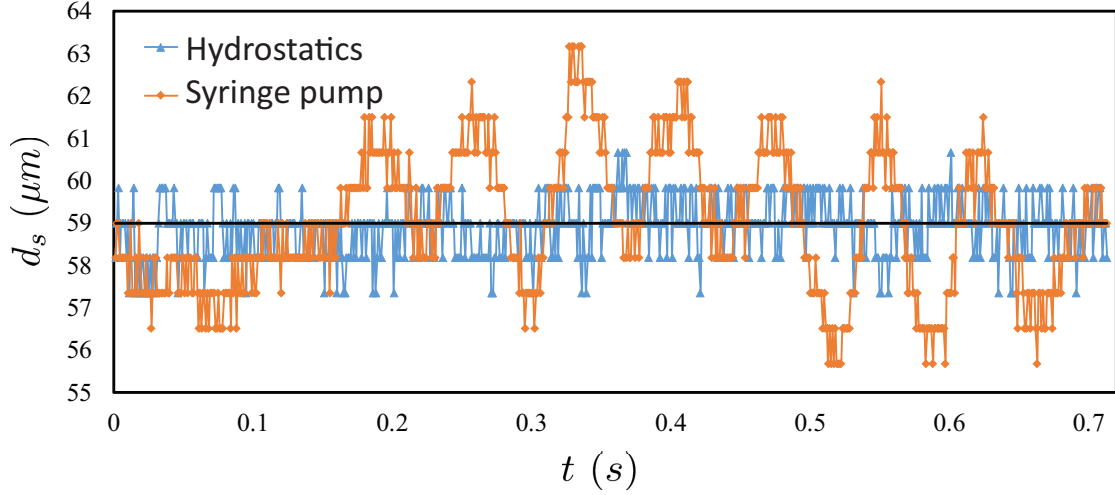
FIG. 3. A plot of the focused flow diameter, d_s, versus time, t, for experiments using hydrostatic pressure (blue triangle) and syringe pumps (red diamond) over a period $\Delta t = 0.7$ s. The average diameter, d_s, of the focused flow in both hydrostatics and syringe-pump experiments is $d_s = 59$ μm (indicated by the black line). $t = 0$ s represents the first frame of the high speed video. The data shows significantly larger fluctuations in the syringe pump experiments.

experiments, we record videos for a duration of 0.7 s at a frame rate of 1,000 fps, and for the syringe pump experiments the videos are recorded for a duration of 16 s at frame rate of 200 fps.

The curves in Fig. 4 show that the cumulative normal distributions of the focused flow diameter in the hydrostatics experiments are consistently narrower for all of the experiments. The distributions of the focused flow diameter in the pump experiments are inconsistent and do not show any specific trend in the narrowness of the flow. For example, the experiments with $d_s/w = 0.140$ show that the distributions of the syringe pump and hydrostatics experiments are nearly the same, while for $d_s/w = 0.100$ the pump experiment results in a significantly wider distribution than the hydrostatics experiment. These results suggest that the hydrostatic flow focusing technique is better than focusing a flow using syringe pumps for sensitive applications that require accurate and consistent focused flows. We also find that the hydrostatics-based system maintains a near constant focused flow diameter, d_s, for at least several minutes into each experiment, before increasing due to changes to the liquid column heights of the sample and sheath fluids with time (see details in Supplementary
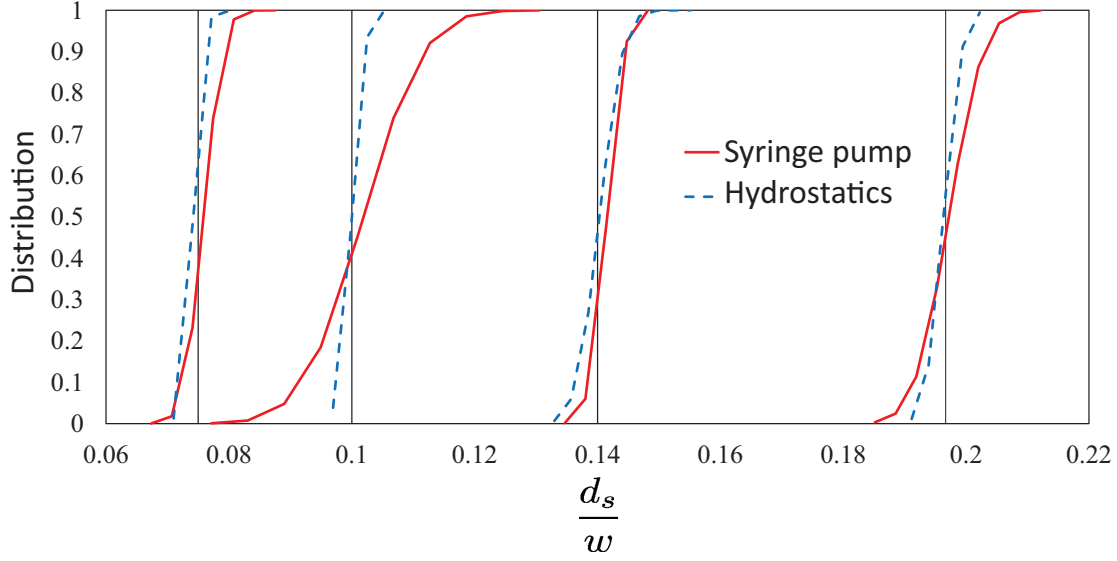
8

FIG. 4. A plot of the cumulative normal distribution function versus dimensionless focused flow diameter, d_s/w, in the microfluidic channel driven by hydrostatic pressure (blue dashed lines) and syringe pumps (red solid lines). The four sets of data correspond to averaged focused flow widths, $d_s/w = 0.075$, 0.100, 0.140 and 0.197 (from left to right). Hydrostatics-controlled flows show consistently narrower distributions of the focused width, d_s/w, compared to the focused flow generated by syringe pumps.

Information). We note that these changes could be reduced by continually filling the liquid columns with liquid, or by increasing the diameter of the liquid columns. The liquid columns can be continuously supplied with liquid using a liquid reservoir connected to the columns. Alternatively, a continuous liquid supply can be achieved by using a syringe pump to infuse the liquid at a flowrate equal to the rate at which the column is discharging liquid to the microfluidic device. These methods may help to maintain constant fluid column heights.

B.   Controlling hydrostatics based flow focusing

In syringe-pumped based flow focusing systems, the focused sample flow diameter scales as,[26]
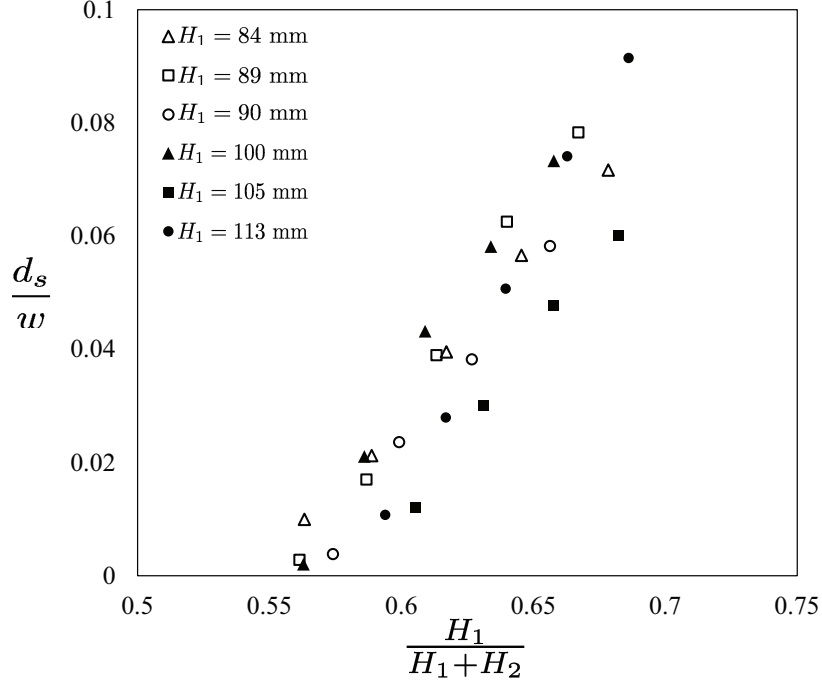
$$\frac{d_s}{w} \propto \frac{Q_1}{Q_1 + Q_2},$$ (1)

9

FIG. 5. A plot of the dimensionless focused sample flow diameter, d_s/w, versus the ratio of liquid column heights, $\dfrac{H_1}{H_1 + H_2}$. Here, the data shows results from six experiments where the sample liquid column height, $H_1 = 84$, 89, 90, 100, 105, and 113 mm, and the sheath flow liquid column height, H_2, is varied to achieve different focused sample flow diameters, d_s/w. The results indicate monotonic and approximately proportional increase of the focused sample flow diameter, d_s/w, with the ratio of liquid column heights, $\dfrac{H_1}{H_1 + H_2}$, suggesting that the parameter $\dfrac{H_1}{H_1 + H_2}$ is a good controller for the degree of hydrostatics based flow focusing.

where Q_1 and Q_2 are the sample and sheath fluid flow rates, respectively. The Poiseuille flow relationship has a linear proportionality between the flow rate, Q, and the pressure drop, ΔP, such that $Q \propto \Delta P$. Hydrostatics dictates that the pressure drop, ΔP, scales linearly with the height, H, of a liquid column. Therefore, our hydrostatically flow focused sample fluid will have a resulting normalized diameter,

$$\frac{d_s}{w} \propto \frac{H_1}{H_1 + H_2}. \tag{2}$$

Fig. 5 shows the dimensionless focused sample flow diameter d_s/w, plotted against the ratio of liquid column heights, $\dfrac{H_1}{H_1 + H_2}$. Here, in six experiments, we fix the sample fluid's liquid column height $H_1 = 84, 89, 90, 100, 105,$ and 113 mm, and tune the sheath flow column height, H_2, to obtain a range of dimensionless focused sample flow diameters d_s/w. In all of the experiments, we observe that the sample flow diameter, d_s, is approximately proportional to the parameter $\dfrac{H_1}{H_1 + H_2}$. Therefore, these results suggest that the sample flow diameter, d_s, is directly controllable by simply adjusting the ratio $\dfrac{H_1}{H_1 + H_2}$.

IV. CONCLUSION

In this work, we describe a stable hydrostatic pressure actuated hydrodynamically focused flow in a single layer microfluidic device. We validate the stability of the focused flow by comparing our results with values from conventional syringe pump actuated flow focusing. Overall, our results show that hydrostatics actuated flow focusing is more stable than syringe pump based flow focusing.

Additionally, we find that hydrostatic based focused flow diameter, d_s, is easily adjustable by tuning the ratio of the heights of the liquid columns, $\dfrac{H_1}{H_1 + H_2}$, which enables simple control by changing a single parameter. We expect that the stability and ease-of-control of this flow focusing technique will make it highly useable in a variety of microfluidic flow cytometer systems.

V. SUPPLEMENTARY MATERIAL

See supplementary matarial for more information on hydrostatic experiment on controlled focus flow diameter and for a confocal microscopy video showing an axis-symmetric effect on the focused flow in both lateral (x-y) and vertical (x-z) axes.

VI. ACKNOWLEDGEMENT

REFERENCES

[1] P. A. Auroux, D. Iossifidis, D. R. Reyes, and A. Manz, Analytical Chemistry **74**, 2637 (2002).

[2] A. Manz, H. M. Widmers, and N. Graber, Sensors and Actuators B: Chemical **1**, 244 (1990).

[3] D. Mark, S. Haeberle, G. Roth, F. von Stetten, and R. Zengerle, Chemical Society Reviews **39**, 1153 (2010).

[4] L. J. Millet, J. D. Lucheon, R. F. Standaert, S. T. Rettererab, and M. J. Doktyczab, Lab on a Chip **15**, 1799 (2015).

[5] H. A. Stone, A. D. Stroock, and A. Ajdari, Annual Review of Fluid Mechanics **36**, 381 (2004).

[6] S.-I. Pai, *Viscous Flow Theory: Laminar Flow* (1956).

[7] J. Ducree and R. Zengerle, *Microfluidics* (2004) p. 520.

[8] A. S. Yang and W. H. Hsieh, Biomedical Microdevices **9**, 113 (2007).

[9] G.-B. Lee, C.-I. Hung, B.-J. Ke, G.-R. Huang, B.-H. Hwei, and H.-F. Lai, Journal of Fluids Engineering **123**, 672 (2001).

[10] J. V. Watson, *Introduction to Flow Cytometry* (Cambridge University Press, 2004).

[11] M. Brown and C. Wittwer, Clinical Chemistry **8**, 1221 (2000).

[12] S. Gawad, L. Schild, and P. H. Renaud, Lab on a Chip **1**, 76 (2001).

[13] T. Sun and H. Morgan, Microfluidics and Nanofluidics **8**, 423 (2010).

[14] Q. Xu, M. Hashimoto, T. T. Dang, T. Hoare, D. S. Kohane, G. M. Whitesides, R. Langer, and D. G. Anderson, Small **02115**, 1575 (2009).

[15] P. S. Dittrich and A. Manz, Nature Reviews Drug Discovery **5**, 210 (2006).

[16] P. K. Wong, Y.-K. Lee, and C.-M. Ho, Journal of Fluid Mechanics **497**, 55 (2003).

[17] J. Knight, A. Vishwanath, J. Brody, and R. Austin, Physical Review Letters **80**, 3863 (1998).

[18] T. Ward, M. Faivre, M. Abkarian, and H. A. Stone, Electrophoresis **26**, 3716 (2005).

[19] Z. Li, S. Y. Mak, A. Sauret, and H. C. Shum, Lab on a Chip , 744 (2014).

[20] W. Zeng, I. Jacobi, D. J. Beck, S. Li, and H. A. Stone, Lab on a Chip **15**, 1110 (2015).

[21]J. Atencia and D. J. Beebe, Lab on a Chip **6**, 567 (2006).

[22]X. Mao, S.-C. S. Lin, C. Dong, and T. J. Huang, Lab on a Chip **9**, 1583 (2009).

[23]E. M. Strohm, V. Gnyawali, M. Van De Vondervoort, Y. Daghighi, S. S. H. Tsai, and M. C. Kolios, in *Proceedings of SPIE*, Vol. 9708 (2016) p. 97081A.

[24]Y. Xia and G. M. Whitesides, Annual Review of Materials Science **28**, 153 (1998).

[25]N. Otsu, Automatica **11**, 23 (1975).

[26]T. Stiles, R. Fallon, T. Vestad, J. Oakey, D. Marr, J. Squier, and R. Jimenez, Microfluidics and Nanofluidics **1**, 280 (2005).